Inorg. Chem. **2009**, *48*, 2770−2779

Copper(II) Interaction with Mono-, Bis- and Tris-Ring N_3O_2 Macrocycles: Synthetic, X-ray, Competitive Membrane Transport, and Hypochromic Shift Studies

Joobeom Seo,[†] Sunhong Park,[†] Shim Sung Lee,*[,†] Marina Fainerman-Melnikova,[‡] and Leonard F. Lindoy*[,‡]

Department of Chemistry (BK21) and Research Institute of Natural Science, Gyeongsang National University, Jinju 660-701, S. Korea, and Centre for Heavy Metal Research, School of Chemistry, F11, The University of Sydney, NSW 2006, Australia

Received July 7, 2008

New *N*-phenyl (**L**[1]), azo-coupled (**L**[2]), and tri-linked (**L**[3]) substituted derivatives of a parent dibenzo-N_3O_2 macrocycle, 1,12,15-triaza-3,4:9,10-dibenzo-5,8-dioxacycloheptadecane (**L**[4]), have been synthesized. Competitive seven-metal transport studies across a bulk chloroform membrane employing an aqueous source phase containing equal molar concentrations of Co(II), Ni(II), Cu(II), Zn(II), Cd(II), Ag(I), and Pb(II) as their nitrate salts have been performed using both **L**[1] and **L**[3] as the ionophore, with the results discussed in terms of those obtained previously for related mono-ring (**L**[5]) and di-linked (**L**[6]) macrocyclic systems. Sole transport selectivity for Cu(II) was observed in each case. On a per macrocyclic cavity basis the tri-linked analogue **L**[3] gave less efficient Cu(II) transport than its monomeric or di-linked analogues. At least in part, this may reflect the tendency of tri-linked derivative **L**[3] to form a 2:1 complex (metal/ligand) with Cu(II) under the conditions employed; such a stoichiometry was demonstrated to occur in acetonitrile using both spectrophotometric titration and Job plot procedures. The azo-coupled derivative (**L**[2]) yields a red solution ($\lambda_{max} = 495$ nm, $\varepsilon_{max} = 23000$ M^{-1} cm^{-1}) and undergoes significant hypochromic metal-induced shifts ($\Delta\lambda_{max} = 54-174$ nm) on metal addition. Cu(II) induces the largest shift ($\Delta\lambda_{max} = 174$ nm), corresponding to a color change from red to pale-yellow. The X-ray structures of red **L**[2]$\cdot HNO_3$ together with its Cu(II) complexes, $[Cu(\mathbf{L}^2)NO_3]NO_3 \cdot CH_2Cl_2$ (**6**) (pale-yellow) and $[\{Cu(\mathbf{L}^2)\}_2(\mu\text{-}OH)_2](ClO_4)_2 \cdot 2CH_2Cl_2 \cdot 2H_2O$ (**7**) (dark-red), are reported. The structural determinations have allowed insight into the structure−function relationships governing the observed color variation between these species.

Introduction

Related to the presence of a central cavity, macrocycles have long been employed in investigations of metal ion recognition.[1] In this context, we have investigated the selective behavior of a range of dibenzo-substituted, mixed donor macrocyclic systems toward a range of transition and post-transition metal ions.[2,3] Such ligands have been demonstrated to form complexes with a wide range of transition and post-transition metal ions. In these studies systematic variation of the macrocyclic ring size, the donor atom set, and the substituents on the ring have all been employed to "tune" such ring systems for selective metal ion recognition.[2] In an extension of these studies we now present a comparative investigation of aspects of the complexation behavior of the new cyclic derivatives **L**[1], **L**[2], and **L**[3] toward selected transition and post-transition metal ions. The results are compared with those obtained previously[3c] from parallel studies for the parent N_3O_2-macrocycle **L**[4] and the related substituted derivatives **L**[5] and **L**[6] (see Chart 1). Structure/

* To whom correspondence should be addressed. E-mail: sslee@gnu.ac.kr (S.S.L.), lindoy@chem.usyd.edu.au (L.F.L.).
[†] Gyeongsang National University.
[‡] The University of Sydney.

(1) Gloe, K. *Macrocyclic Chemistry: Current Trends and Future*; Springer: Dordrecht, 2005.

(2) (a) Adam, K. R.; Antolovich, M.; Baldwin, D. S.; Brigden, L. G.; Duckworth, P. A.; Lindoy, L. F.; Bashall, A.; McPartlin, M.; Tasker, P. A. *J. Chem. Soc., Dalton Trans.* **1992**, 1869. (b) Adam, K. R.; Arshad, S. P. H.; Baldwin, D. S.; Duckworth, P. A.; Leong, A. J.; Lindoy, L. F.; McCool, B. J.; McPartlin, M.; Tailor, B. A.; Tasker, P. A. *Inorg. Chem.* **1994**, *33*, 1194. (c) Adam, K. R.; Baldwin, D. S.; Duckworth, P. A.; Lindoy, L. F.; McPartlin, M.; Barshall, A.; Powell, H. R.; Tasker, P. A. *J. Chem. Soc., Dalton Trans.* **1995**, 1127.

10.1021/ic801265y CCC: $40.75
Published on Web 03/09/2009

Chart 1. Mono-, Bis-, and Tris-Ring N_3O_2 Macrocycles

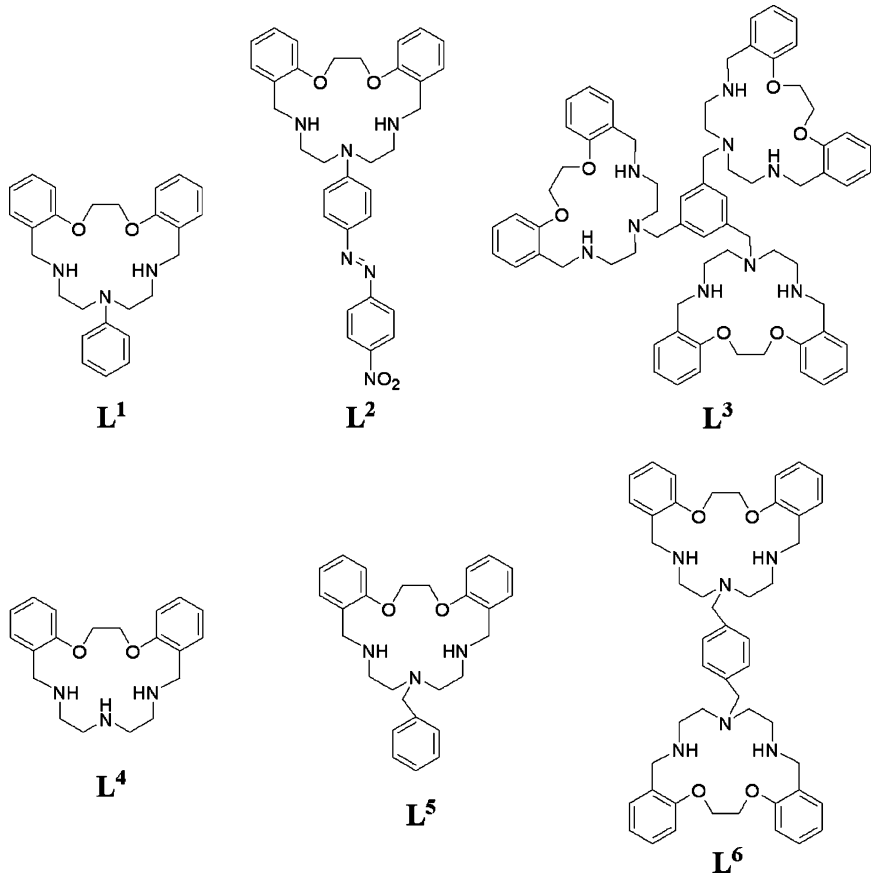

function relationships underlying the metal induced color changes of $\mathbf{L}^2$, obtained by attaching a chromophoric benzoazo substituent to the central amine group of the parent macrocycle $\mathbf{L}^4$, are also discussed.

Experimental Section

General Procedures. NMR spectra were recorded on a Bruker Avance 300 spectrometer (300 MHz) and mass spectra were obtained on a JEOL JMS-700 spectrometer at the Central Laboratory of Gyeongsang National University. The UV−vis absorption spectra were recorded with a Cary 5E (Varian) or a Scinco S-3100 spectrophotometer. Infrared spectra were measured with a Mattson Genesis Series FT-IR spectrophotometer. Microanalyses were performed by an Elemental Analysen Systeme Vario EL at the KBSI (Daegu, S. Korea).

Ligand $\mathbf{L}^1$. 4-Phenyl-diethylenetriamine[4] (0.90 g, 5.02 mmol) in methanol (50 mL) was slowly added to a stirred solution of 1,4-bis(2-formylphenyl)-1,4-dioxabutane[5] (1.36 g, 5.03 mmol) in methanol (200 mL). The solution was refluxed for 1 h, and then sodium borohydride (0.57 g, 15.1 mmol) was slowly added to the stirred solution. After the reaction had ceased, the solution was cooled and then filtered. On addition of ice to the filtrate, an oil separated, which was extracted into dichloromethane. The combined organic phases were dried over anhydrous sodium sulfate and evaporated to yield $\mathbf{L}^1$ as a yellow glassy solid (1.05 g. 50%). Mp: 59−61 °C, IR (KBr, cm^{-1}): 3323(m), 2925(w), 1599(m), 1506(m), 1450(m), 1363(m), 1232(s), 1126(m), 1063(w), 937(w), 750(w). MS (ESI): m/z = 418.1 [$(M+1)^+$, $(C_{26}H_{31}N_2O_2+H)^+$], ^{1}H NMR (300 MHz, $CDCl_3$) δ 7.20−6.65 (m, 13H, aromatic H), 4.27 (s, 4H, CH_2O), 3.98 (br, 2H, NH), 3.85 (s, 4H, $ArCH_2$), 3.39 (t, J 5.3 Hz, 4H, NCH_2), 2.74 (t, J 5.3 Hz, 4H, NCH_2CH_2). ^{13}C-{^{1}H} NMR (75 MHz, $CDCl_3$): 156.9, 148.7, 131.2, 129.0, 128.8, 127.7, 121.3, 118.7, 115.9, 112.2, 67.2, 53.0, 49.2, 46.6. Anal. Calcd for $C_{26}H_{31}N_3O_2$: C, 74.79; H, 7.48; N, 10.06. Found: C, 74.98; H, 7.78; N, 9.84%.

Di-Boc-Protected Macrocycle 1. Di-*tert*-butyl dicarbonate (2.36 g, 10.8 mmol) was added to a stirred solution of $\mathbf{L}^1$ (1.81 g, 4.33 mmol) in dichloromethane (100 mL). The solution was stirred at room temperature for 30 min and then evaporated to give yellow oil. Flash column chromatography on silica gel using 10% ethyl acetate/*n*-hexane as the eluent led to the isolation of **1** as a white solid (2.41 g, 90%). ^{1}H NMR (300 MHz, $CDCl_3$) δ 7.28−6.62 (m, 13H, aromatic H), 4.59 (s, 4H, CH_2O), 4.42 (s, 4H, CH_2O), 3.34−3.28 (br, 8H, NCH_2CH_2), 1.53 (s, 9H, *t*-Bu), 1.46 (s, 9H, *t*-Bu). ^{13}C-{^{1}H} NMR (75 MHz, $CDCl_3$): 156.4, 148.4, 129.3, 128.7, 128.4, 126.3, 121.5, 120.9, 116.16, 111.4, 110.9, 80.1, 67.3, 47.7, 43.8, 43.1, 28.5. HRMS (EI): Calcd for $C_{36}H_{47}N_3O_6$ (M^+): 617.3465. Found: 617.3470.

Di-Boc-Protected Marocycle 2. A diazonium salt of 4-nitroaniline (0.20 g, 1.44 mmol) was prepared by adding an aqueous solution of sodium nitrite (0.13 g, 1.87 mmol) dropwise into a homogeneous mixture of sulfuric acid (0.3 mL) and glacial acetic

(3) (a) Fenton, R. R.; Gauci, R.; Junk, P. C.; Lindoy, L. F.; Luckay, R. C.; Meehan, G. V.; Price, J. R.; Turner, P.; Wei, G. *J. Chem. Soc., Dalton Trans.* **2002**, 2185. (b) Jin, Y.; Yoon, Il.; Seo, J.; Lee, J.-E.; Moon, S.-T.; Kim, J.; Han, S. W.; Park, K.-M.; Lindoy, L. F.; Lee, S. S. *Dalton Trans.* **2005**, 788. (c) Fainerman-Melnikova, M.; Nezhadali, A.; Rounaghi, G.; McMurtrie, J. C.; Kim, J.; Gloe, K.; Langer, M.; Lee, S. S.; Lindoy, L. F.; Nishimura, T.; Park, K.-M.; Seo, J. *Dalton Trans.* **2004**, 122.
(4) Ueda, T.; Kobayashi, S. *Chem. Pharm. Bull.* **1969**, *17*, 1720.
(5) Armstrong, L. G.; Grimsley, P. G.; Lindoy, L. F.; Lip, H. C.; Norris, V. A.; Smith, R. J. *Inorg. Chem.* **1978**, *17*, 2350.

acid (1 mL). The mixture was stirred at 0 °C for 5 min. The diazonium salt solution was added dropwise to a solution of **1** (0.69 g, 1.12 mmol) in *N*,*N*-dimethylformamide at 0 °C. The solution was stirred for 12 h at 0 °C. Dichloromethane (50 mL) and water (50 mL) were added, and the organic layer was separated and dried over anhydrous sodium sulfate. Removal of the organic solvent under reduced pressure afforded a reddish oil. Flash column chromatography on silica gel using 20% ethyl acetate/*n*-hexane as the eluent led to the isolation of **2** as a pink solid (0.69 g, 80%). ^{1}H NMR (300 MHz, $CDCl_3$) δ 8.33−6.80 (m, 16H, aromatic H), 4.62 (s, 2H, CH_2O), 4.40 (s, 2H, CH_2O), 4.40 (s, 4H, $ArCH_2$), 3.46−3.34 (br, 8H, NCH_2CH_2), 1.53 (s, 9H, *t*-Bu), 1.50 (s, 9H, *t*-Bu). ^{13}C-{^{1}H} NMR (75 MHz, $CDCl_3$): 156.8, 156.6, 156.2, 152.6, 147.6, 144.0, 130.0, 129.0, 126.9, 126.2, 125.0, 122.8, 121.7, 111.8, 111.0, 67.8, 67.0, 48.6, 44.8, 42.9, 28.8. HRMS (EI): Calcd. for $C_{42}H_{50}N_6O_8$ (M^+): 766.3690. Found: 766.3694.

Ligand L^2. Protected intermediate **2** (0.69 g, 0.90 mmol) was added to a stirred mixture of dichloromethane (30 mL) and trifluoroacetic acid (30 mL) and stirring was continued at room temperature for 2 h. The solvent was removed using a rotary evaporator, methanol was added to the residue, and the resulting solution again taken to dryness. This procedure was repeated three times to remove any remaining trifluoroacetic acid. Aqueous sodium carbonate (15%, 50 mL) was added to the residue, and the mixture extracted with dichloromethane three times. The combined organic phases were dried over anhydrous sodium sulfate and evaporated to yield **L**^{2} as a reddish glassy solid (0.46 g, 90%). MS (ESI): ^{1}H NMR (300 MHz, $CDCl_3$) δ 8.33−6.62 (m, 16H, aromatic H), 4.31 (s, 4H, CH_2O), 3.98 (s, 4H, $ArCH_2$), 3.83 (br, 4H, NCH_2), 2.98 (br, 4H, NCH_2CH_2), 2.53 (br, 2H, NH). ^{13}C-{^{1}H} NMR (75 MHz, $CDCl_3$): 157.3, 157.0, 148.0, 144.6, 142.4, 132.1, 130.0, 126.4, 125.1, 123.1, 122.6, 114.3, 112.4, 68.5, 52.0, 48.5, 46.4. HRMS (EI): Calcd for $C_{32}H_{34}N_6O_4$ (M^+): 566.2642. Found: 566.2630.

Di-Boc Protected Macrocycle 3. This was obtained by direct Boc-protection of **L**^{4} followed by purification via column chromatography as described previously.[6]

Boc-Protected Precursor 4. 1,3,5-Benzenetricarbonyl trichloride (0.16 g, 0.60 mmol) in acetonitrile (40 mL) was added dropwise to a refluxing suspension of **3** (1.12 g, 2.06 mmol) and potassium carbonate (2.57 g, 18.50 mmol) in acetonitrile (150 mL). The reaction mixture was then maintained at reflux for an additional 24 h with rapid stirring, allowed to cool to room temperature and filtered. The filtrate was evaporated on a rotary evaporator, and the residue was partitioned between water and dichloromethane. The aqueous phase was separated and extracted with two further portions of dichloromethane. The combined organic phases were dried over anhydrous sodium sulfate, and the solution then evaporated to dryness. Flash column chromatography on silica gel using 70% ethyl acetate/*n*-hexane as the eluent led to the isolation of **4** as a white solid (0.97 g. 92%). Mp: 135−138 °C, IR (KBr, cm^{-1}): 3065(m), 2974(m), 2932(s), 2877(m), 2359(w), 2335(w), 1693 (s, $\nu_{C=O}$), 1644(m), 1597(w), 1486(m), 1455(m), 1413(m), 1365(m), 1241(w), 1158(m), 1126(w), 1051(m), 933(m), 888(w), 811(w), 752(w), 611(w), 552(w), 438(w). ^{1}H NMR (300 MHz, $CDCl_3$): 7.24−6.89 (m, 27H, aromatic), 4.55 (br, 12H, CH_2O), 4,35 (br, 12H, $ArCH_2$), 3.75−3.13 (br, 24H, NCH_2CH_2), 1.60−1.26 (br, 54 H, $C(CH_3)_3$), ^{13}C-{^{1}H} NMR 170.9, 156.2, 128.3, 127.7, 126.4, 121.3, 110.9, 79.5, 67.1, 60.3, 48.9, 46.8, 45.0, 43.5, 28.4, 21.0, 14.2. Pronounced broadening and/or splitting of signals in the ^{1}H and ^{13}C NMR spectra of this compound were observed. HRMS (FAB): Calcd for $C_{99}H_{130}N_9O_{21}$ ($M+H^+$): 1780.9381. Found: 1780.9281.

Triamide 5. The protected triamide **4** (1.18 g, 0.65 mmol) was added to a stirred mixture of dichloromethane (30 mL) and trifluoroacetic acid (30 mL). The reaction mixture was stirred at room temperature for 2 h. After removal of the solvent in a rotary evaporator, methanol was added and then evaporated again to dryness. Aqueous sodium carbonate (15%, 50 mL) was added to the residue, and this mixture was extracted with dichloromethane three times. The combined organic phases were dried over anhydrous sodium sulfate, and the solvent removed to yield triamide **5** as a pale yellow glassy solid (0.69 g, 90%). Mp: 112−115 °C, IR (KBr, cm^{-1}): 2932(m), 1624(s, $\nu_{C=O}$), 1468(m), 1236(m), 1113(s), 933(w), 756(w). MS (ESI): m/z = 1180.8 ($[M+1]^+$, $[C_{69}H_{81}N_9O_9+H]^+$), ^{1}H NMR (300 MHz, $CDCl_3$): 7.41−6.88 (m, 27H, aromatic), 4.40 (s, 6 H, CH_2O), 4,36 (s, 6H, CH_2O), 3.85 (s, 6H, $ArCH_2$), 3.73 (s, 6H, $ArCH_2$), 3.56 (s, 6H, NCH_2), 3.30 (s, 6H, NCH_2), 2.88 (m, 6H, $NHCH_2CH_2$), 2.65 (m, 6H, $NHCH_2CH_2$). ^{13}C-{^{1}H} NMR 157.1, 135.8, 131.1, 129.8, 128.8, 128.5, 120.8, 111.2, 67.1, 54.8, 50.2, 48.5. Pronounced broadening and/or splitting of signals in the ^{1}H and ^{13}C NMR spectra of this compound were observed. HRMS (FAB): Calcd for $C_{69}H_{82}N_9O_9$ ($M+H^+$): 1180.6236. Found: 1180.6298.

Ligand L^3. A solution of $BH_3\cdot Me_2S$ complex (2.0 M; 2.23 mL, 4.46 mmol) was added to triamide **5** (0.87 g, 0.73 mmol) in dry THF (50 mL) at 60 °C. The reaction mixture was stirred until no carbonyl absorption could be observed by IR spectroscopy (ca. 6 h). Excess borane was destroyed by careful addition of methanol, and the solvent was removed under reduced pressure. The residual white powder was then refluxed in MeOH-H_2O-conc.HCl (20:5:2, 27 mL) for 1.5 h. The methanol was evaporated under reduced pressure, and the aqueous residue basified with 10% aqueous sodium hydroxide (100 mL). The basic solution was extracted with CH_2Cl_2 and then the combined organic extracts dried and evaporated to yield **L**^{3} as a white glassy solid (0.74 g, 90%). IR (KBr, cm^{-1}): 3310(m), 2924(m), 1450(m), 1238(m), 1109(s), 943(w), 752(w). ^{1}H NMR (300 MHz, $CDCl_3$) 7.26−6.44 (m, 27H, aromatic H), 4.38 (s, 12H, CH_2O), 3.79 (s, 12H, $ArCH_2NH$), 3.41 (br, 6H, NH), 3.12 (s, 6H, NCH_2Ar), 2.59 (m, 12H, NCH_2CH_2), 2.36 (m, 12H, $NHCH_2CH_2$). ^{13}C-{^{1}H} NMR (75 MHz, $CDCl_3$) 157.1, 136.6, 131.4, 129.8, 128.9, 127.9, 121.2, 111.8, 67.2, 52.5, 49.7, 45.7. Pronounced broadening of signals in the ^{1}H and ^{13}C NMR spectra of this compound was observed. HRMS (FAB): Calcd for $C_{69}H_{88}O_6N_9$ ($M+H^+$) 1138.6858: Found: 1138.6855.

Synthesis of Cu(II) Complexes of L^2. Toluene (0.4 mL) was added to a dichloromethane solution (1.0 mL) of **L**^{2} (20 mg, 0.035 mmol); then the required Cu(II) salt (nitrate for **6** and perchlorate for **7**; 0.035 mmol) in methanol was layered on the toluene phase; the (layered) mixture was allow to stand for 2 weeks during which time crystalline complexes suitable for X-ray analysis formed at the interface. Isolated yields were greater than 30%.

[Cu(L^2)NO$_3$]NO$_3\cdot$CH$_2$Cl$_2$ (6). Yellow crystals. IR (KBr, cm^{-1}): 3421(m), 1601(s), 1514(m), 1452(m), 1385(s), 1339(s), 1244(m), 1132(m), 955(w), 858(w), 756(w). MS (FAB): m/z = 691.25 ($[Cu(\mathbf{L}^2)NO_3]^+$, $[C_{32}H_{34}CuN_7O_7]^+$). HRMS (FAB): Calcd. for $C_{32}H_{34}CuN_7O_7$ ($[Cu(\mathbf{L}^2)NO_3]^+$): 691.1816. Found: 691.1813.

[{Cu(L^2)}$_2$(μ-OH)$_2$](ClO$_4$)$_2\cdot$2CH$_2$Cl$_2\cdot$2H$_2$O (7). Red crystals. IR (KBr, cm^{-1}): 3566(m), 1601(s), 1522(m), 1454(m), 1336(s), 1245(m), 1105(s, ν_{ClO4}), 858(w), 756(w), 624(w).

X-ray Crystallographic Analysis. Crystals of the respective products were mounted on a Bruker SMART diffractometer equipped with a graphite monochromated Mo Kα (λ = 0.71073

(6) (a) Chartres, J. D.; Groth, A. M.; Lindoy, L. F.; Lowe, M. P.; Meeham, G. V. *J. Chem. Soc., Perkin Trans. 1.* **2000**, 3444. (b) Park, K. J.; Kim, J.-H.; Meehan, G. V.; Nishimura, T.; Lindoy, L. F.; Lee, S. S.; Park, K.-M.; Yoon, I. *Aust. J. Chem.* **2002**, *55*, 773.

Table 1. Crystal Data and Structural Refinement

	$\mathbf{L}^1 \cdot HNO_3 \cdot HPF_6 \cdot CH_3OH \cdot H_2O$	**6**	**7**
formula	$C_{27}H_{39}F_6N_4O_{6.50}P$	$C_{33}H_{34}Cl_2CuN_8O_{10}$	$C_{66}H_{70}Cl_6Cu_2N_{12}O_{19}$
M	668.59	837.12	1675.12
T/K	173(2)	173(2)	173(2)
crystal system	monoclinic	triclinic	monoclinic
space group	*C*2/*c*	$P\bar{1}$	$P2_1/n$
a/Å	14.7378(8)	8.2961(6)	15.1258(7)
b/Å	18.4875(10)	12.8519(10)	15.6145(7)
c/Å	23.8503(13)	17.9321(13)	16.5997(8)
α/deg		77.861(2)	
β/deg	100.2780(10)	82.893(2)	106.7310(10)
γ/deg		78.241(2)	
V/Å^3	6394.1(6)	1823.4(2)	3754.6(3)
Z	8	2	2
μ(Mo Kα)/mm^{-1}	0.168	0.814	0.859
crystal size (mm)	0.20 × 0.20 × 0.15	0.10 × 0.05 × 0.04	0.10 × 0.10 × 0.05
absorption correction	SADABS	SADABS	SADABS
reflections collected	20129	11279	21079
independent reflections	7504	7756	7338
goodness-of-fit on F^2	1.086	1.073	1.012
final *R*1, *wR*2 [$I > 2\sigma(I)$]	0.1249, 0.3080	0.0822, 0.2004	0.0750, 0. 0.2020
(all data)	0.1757, 0.3422	0.1887, 0.2648	0.1428, 0.2523

Å) radiation source, and a CCD detector and 45 frames of two-dimensional diffraction images were collected and processed to deduce the cell parameters and orientation matrix. A total of 1271 frames of two-dimensional diffraction images were collected. The frame data were processed to give structure factors by the program SAINT.[7] The intensity data were corrected for Lorentz and polarization effects. Using the program SADABS,[8] empirical absorption corrections were also applied for compounds $\mathbf{L}^1$, $\mathbf{L}^2$, **1**, **6**, and **7**. The structures were solved by a combination of direct and difference Fourier methods provided by the program package SHELXTL[9] and refined using a full matrix least-squares against F^2 for all data. All the non-H atoms were refined anisotropically. All hydrogen atoms were included in calculated positions with isotropic thermal parameters 1.2 times those of attached atoms. Crystallographic data for $\mathbf{L}^1$, **6**, and **7** are summarized in Table 1.

Bulk Membrane Transport. Bulk membrane transport (water/chloroform/water) experiments employed a "concentric cell" in which the aqueous source phase (10 mL) and receiving phase (30 mL) were separated by a chloroform phase (50 mL). Details of the cell design have been reported.[10] The concentrations of the ligands in the chloroform phase were set at 1.0×10^{-3} M to enable direct comparison of the results with those for $\mathbf{L}^4$ and $\mathbf{L}^5$ given in previous reports[3c,11] (see Supporting Information, Figure S1). In each case hexadecanoic acid (4×10^{-3} M) was also present in the chloroform phase. A major role of the latter is to aid the transport process by providing a lipophilic counterion in the organic phase (after proton loss to the aqueous source phase) for charge neutralization of the metal cation being transported; in this manner the need for uptake of lipophobic nitrate anions into the organic phase is avoided. For each experiment both aqueous phases and the chloroform phase were stirred separately at 10 revolutions min^{-1}; the cell was enclosed by a water jacket and thermostatted at 25 °C. In each case the aqueous source phase (buffered at pH 4.9 ± 0.1; 6.95 mL of 2 M sodium acetate solution and 3.05 mL of 2 M acetic acid made up to 100 mL) contained a mixture of Co(II), Ni(II), Cu(II), Zn(II), Cd(II), Ag(I), and Pb(II) nitrates, each at a concentration of 10^{-2} M. The receiving phase was buffered at pH 3.0 (56.6 mL of 1 M formic acid and 10.0 mL of 1 M sodium hydroxide made up to 100 mL) (Supporting Information, Figure S2). All transport runs were terminated after 24 h, and atomic absorption spectroscopy was used to determine the amount of metal ion transported over this period. The transport fluxes are in mol/24 h and represent mean values measured over 24 h; values in the range $1.5-2.0 \times 10^{-6}$ are of higher uncertainty, and values less than this are within experimental error of zero; the latter have been ignored in the present study. The results are summarized in Table 2.

Table 2. Cu(II) Transport in Seven-Metal Competitive Transport Experiments Across a Bulk Chloroform Membrane Employing $\mathbf{L}^1$ and $\mathbf{L}^3-\mathbf{L}^6$ as Ionophores at 25 °C[a]

ionophore [b,c]	Cu^{II}
$\mathbf{L}^4$ (mono-)	18.8 [d]
$\mathbf{L}^1$ (mono-)	1.8
L^5 (mono-)	4.8[e]
$\mathbf{L}^6$ (di-)	12.7 [e]
$\mathbf{L}^3$ (tri-)	10.2

[a] Within experimental error, sole transport of Cu(II) into the receiving phase was observed for each ionophore. Each value represents the mean obtained from duplicate experiments and are × 10^{-6}. The units are mol/24 h; values less than ~1.5×10^{-6} are within experimental error of zero and have been ignored in the present study; the quoted mean values are ±8% or lower. [b] The concentration of ligand in the organic phase was 1.00×10^{-3} M. [c] In the seven-metal mixture (source phase), the concentration of each metal was 1.00×10^{-2} M. [d] Values from ref 11. [e] Values from ref 3c.

Results and Discussion

Macrocycle Synthesis. The new phenyl-substituted macrocycle $\mathbf{L}^1$ was obtained directly in 50% yield from reaction of 4-phenyl-diethylenetriamine with 1,4-bis(2-formyl)1,4-dioxabutane in methanol followed by sodium borohydride reduction. Synthesis of 4-nitroazobenzene derivative involved three steps starting from $\mathbf{L}^1$ as shown in Scheme 1, with each step proceeding smoothly in reasonable yield. The synthesis of $\mathbf{L}^1$ was carried out by the well established procedure involving double Schiff base condensation in

(7) *SMART, SAINT and XPREP: Area detector control and data integration and reduction software*, Ver. 5.0; Bruker Analytical X-ray Instruments Inc.: Madison, WI, 1998.
(8) Sheldrick, G. M. *SADABS: Empirical absorption and correction software*. University of Göttingen, Institüt für Anorganische Chemie der Universität, Tammanstrasse 4, D-3400 Göttingen, Germany, 1998.
(9) Sheldrick, G. M. *SHELXTL: Programs for crystal structure analysis*, Ver. 5.16; University of Göttingen, Institüt für Anorganische Chemie der Universität: Tammanstrasse 4, D-3400 Göttingen, Germany, 1998.
(10) Chia, P. S. K.; Lindoy, L. F.; Walker, G. W.; Everett, G. W. *Pure Appl. Chem.* **1993**, *65*, 521.
(11) Kim, J.; Leong, A. J.; Lindoy, L. F.; Kim, J.; Nachbaur, J.; Nezhadali, A.; Rounaghi, G.; Wei, G. *J. Chem. Soc., Dalton Trans.* **2000**, 3453.

Scheme 1. Synthesis of $\mathbf{L}^1$ and $\mathbf{L}^2$

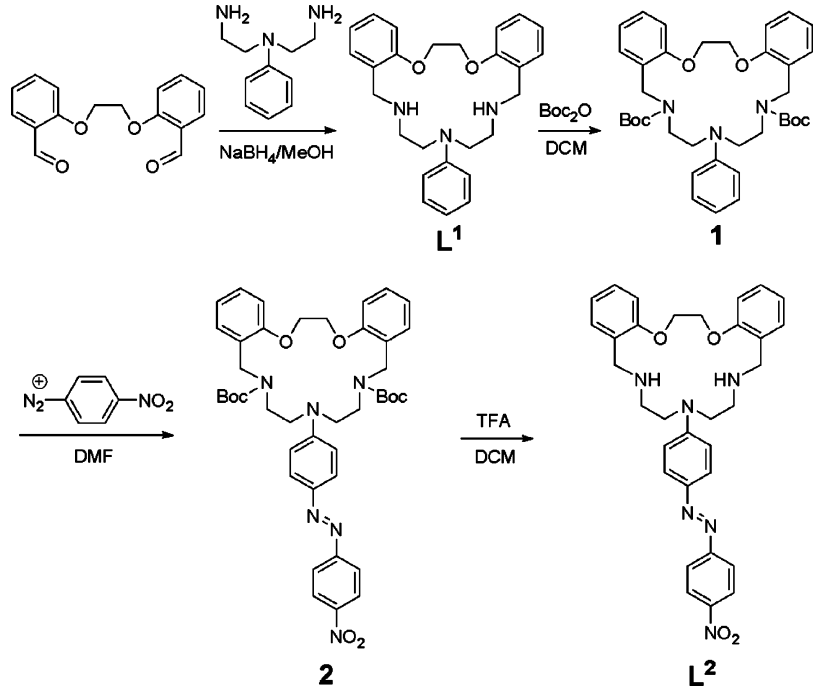

Scheme 2. Synthesis of $\mathbf{L}^3$

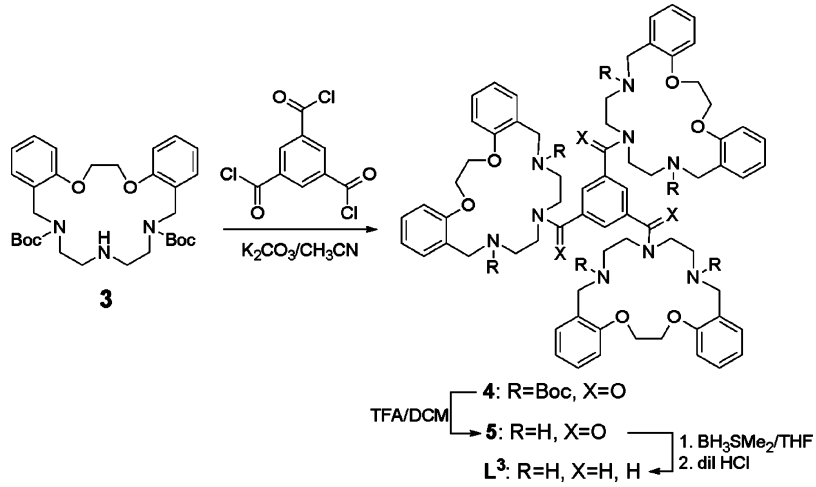

methanol followed by sodium borohydride reduction. *N*-protection by Boc of the two secondary amines of $\mathbf{L}^1$ to yield **1** was then carried out. The di-Boc-protected azo-macrocycle **2** was obtained via exclusive azo formation at the *para*-position of pendant phenyl group of **1** by reaction with 4-nitroaniline under acidic conditions. Removal of the Boc groups of **2** by treatment with trifluoroacetic acid gave the desired azo-coupled derivative $\mathbf{L}^2$.

The synthesis of $\mathbf{L}^3$ is summarized in Scheme 2. The symmetric di-Boc protected derivative **3** was prepared as described previously.[6,12] Reaction of slightly more than 3 equiv of **3** with 1,3,5-benzenetricarbonyl trichloride in acetonitrile in the presence of potassium carbonate afforded the tri-linked, *N*-protected macrocyclic species **4** in 92% yield. Deprotection (using trifluoroacetic acid) of **4** to give the triamide **5** followed by reduction ($BH_3 \cdot SMe_2$/THF) afforded $\mathbf{L}^3$ in 90% yield.

Membrane Transport. Competitive mixed-metal transport experiments have been carried out using a bulk chloroform membrane incorporating $\mathbf{L}^1$ and $\mathbf{L}^3$ as ionophores. In each case the aqueous source phase contained equimolar concentrations of the nitrate salts of Co(II), Ni(II), Cu(II), Zn(II), Cd(II), Ag(I), and Pb(II) (each at 10^{-2} M) buffered at pH 4.9. The aqueous receiving phase was buffered at pH 3.0. The conditions employed were identical to those used previously for studies incorporating $\mathbf{L}^4$, $\mathbf{L}^5$, and $\mathbf{L}^6$ as the ionophores.[3c,11] The ionophore concentration in the organic phase in each case was 1.00×10^{-3} M. Overall, the transport fluxes for Cu(II) were found to fall in the order $\mathbf{L}^4$ (18.8×10^{-6})[11] > $\mathbf{L}^6$ (12.7×10^{-6})[3c] > $\mathbf{L}^3$ (10.2×10^{-6}) > $\mathbf{L}^5$ (4.8×10^{-6})[3c] > $\mathbf{L}^1$ (1.8×10^{-6}), where the values in parentheses are the transport fluxes in units of mol/24 h. No evidence

(12) Smith, R. M.; Martell, A. E. *Critical Stability Constants*; Plenum: New York, 1975; Vol. 2, amines.

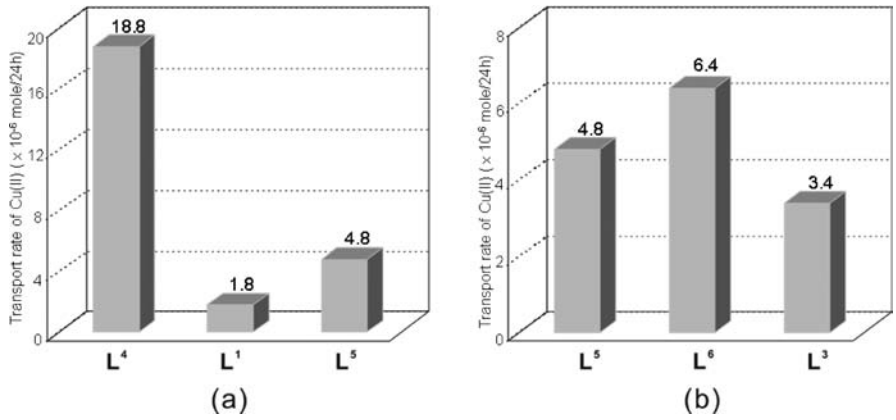

Figure 1. Comparison of the transport rate of Cu(II) for the macrocycles shown. The chloroform phase contained macrocycle at a concentration of 1.0×10^{-3} M and hexadecanoic acid at 4.0×10^{-3} M (see text). The aqueous source phase was buffered at pH 4.9 and contained a mixture of Co(II), Ni(II), Cu(II), Zn(II), Cd(II), Ag(I), and Pb(II) nitrates, each at 1.0×10^{-2} M; (a) the effect of the substituents on the monomeric macrocycles and (b) transport compared on a per-macrocyclic cavity basis on passing from the monomeric ($\mathbf{L}^5$), bis-macrocycle ($\mathbf{L}^6$) to the tris-macrocycle ($\mathbf{L}^3$).

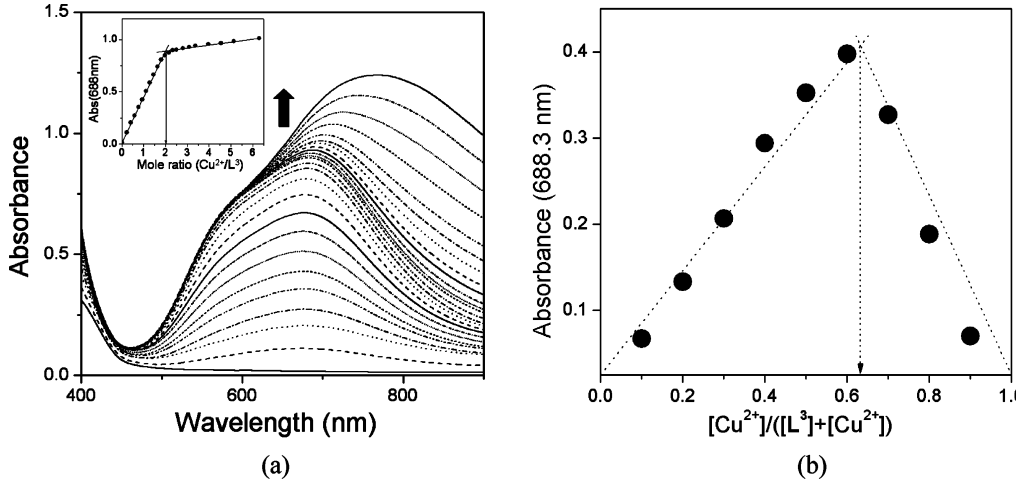

Figure 2. (a) UV−vis titration of $\mathbf{L}^3$ (4.0×10^{-3} M) with Cu(II) nitrate in DMSO (inset: plot of the titration curve) and (b) Job plot for the same complexation system ($[\mathbf{L}^3] = 2.0 \times 10^{-3}$ M) showing 2:1 (M/L) stoichiometry.

for transport of any of the other six metal ions present in the respective source phases was observed under the conditions employed, and thus, sole selectivity for Cu(II) was achieved in each case.

As discussed previously[3c] transport efficiency is influenced by both the strength of the ionophore metal binding and the lipophilicity of the resulting complex in the organic phase. The benzylated derivative $\mathbf{L}^5$ is associated with considerably lower transport efficiency toward copper than found for the parent macrocycle $\mathbf{L}^4$ (Figure 1a). In this case, the transport behavior follows the respective log K data for Cu(II) complexation[3c] even though the overall lipophilicity of the system is expected to be higher for $\mathbf{L}^5$. While no stability data are available for complexation of $\mathbf{L}^1$, the presence of a phenyl substituent will almost certainly further reduce the stability of the corresponding copper complex because of the lower basicity of the substituted anilino amine[12] and perhaps also because of steric influences. In keeping with this, the transport of Cu(II) by $\mathbf{L}^1$ was observed to be significantly lower than occurs for $\mathbf{L}^5$.

It is instructive to compare the results for the tri-linked systems $\mathbf{L}^3$ on a "per macrocyclic hole" basis with those obtained previously[3c] for the benzylated mono-ring derivative

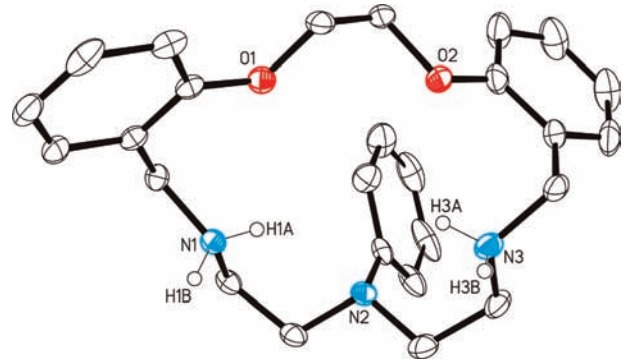

Figure 3. Crystal structure of $\mathbf{L}^1 \cdot HNO_3 \cdot HPF_6 \cdot CH_3OH \cdot H_2O$. Hydrogen atoms (except NH protons), non-coordinating anions and solvents are omitted.

$\mathbf{L}^5$ and its di-linked analogue ($\mathbf{L}^6$) under identical conditions. On this basis, transport efficiency toward Cu(II) is reduced somewhat for the trilinked species (Figure 1b) relative to the other two ring systems. As discussed more fully later, this may reflect the tendency of $\mathbf{L}^3$ to form a 2:1 (M/L) rather than a 3:1 complex with Cu(II); the latter is based on the results from spectrophotometric studies aimed at probing the solution stoichiometry of this system (but it needs to be noted that they were obtained under somewhat different conditions

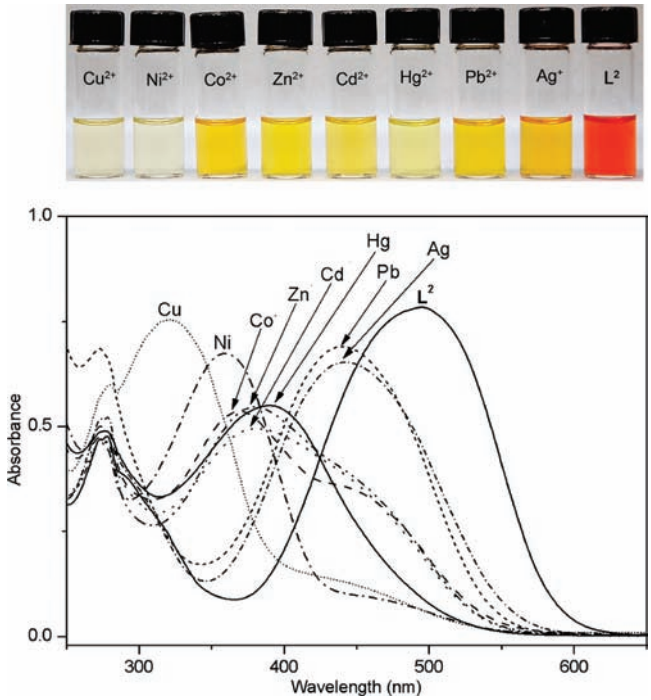

Figure 4. Changes in the UV−vis spectrum of $\mathbf{L}^2$ on addition of the metal nitrates in acetonitrile (ligand concentration, 5.0×10^{-5} M; added metal ion, 3.0 equiv).

to those employed for the membrane transport runs). Nevertheless, from both electrostatic and statistical considerations it is expected that the affinity of $\mathbf{L}^3$ for Cu(II) will be reduced in a stepwise fashion as successive copper ions bind. The situation is further complicated by the observation that, at least in the solid state, there is X-ray evidence that the ether oxygen donors in single-ring macrocycles of the present type tend not to coordinate to Cu(II).[13]

Complexation of Tri-Linked Macrocycle $\mathbf{L}^3$ to Cu(II). In view of the Cu(II) selectivity observed in the membrane transport experiments, the solution complexation of this ion was investigated further. The interaction of $\mathbf{L}^3$ with Cu(II) nitrate in DMSO was examined by means of a UV−vis titration. Incremental addition of $\mathbf{L}^3$ to Cu(II) nitrate in this solvent results in a marked increase in absorbance (maximum = 688.3 nm) up to 2.0 equiv, indicating clear formation of a 2:1 (M/L) species (see inset in Figure 2a). On further addition of ligand the absorption shows little increase at this wavelength (although the λ_{max} then shifts toward longer wavelengths, most likely indicating the gradual conversion of the 2:1 species to a new species that had not completely formed at a ligand/metal ratio of 6.5:1). A Job plot for the interaction of $\mathbf{L}^3$ with Cu(II) nitrate (Figure 2b) yields an absorption maximum that also approximates the formation of a 2:1 (M/L) species under the conditions employed. In contrast to the above behavior, when a ^{1}H NMR titration of $\mathbf{L}^3$ with silver(I) nitrate was carried out in $CDCl_3$/DMSO-d_6 (v/v 1:1) a clear 3:1 ($Ag^+/\mathbf{L}^3$) complex was indicated (Supporting Information, Figure S9).

X-ray Studies of Metal-Free Systems. A mixed anion crystal of $\mathbf{L}^1 \cdot HNO_3 \cdot HPF_6$ suitable for X-ray analysis was obtained by slow evaporation of a dichloromethane solution of $\mathbf{L}^1$ containing several drops of both HNO_3 and HPF_6. The structure of the product (Figure 3) shows that the macrocycle adopts a conformation in which both oxygen donors are directed into the macrocyclic cavity, with the bis-methylene groups between the nitrogen and oxygen donors adopting gauche arrangements. The *N*-phenyl pendant is orientated nearly perpendicular to the ring cavity and shows offset face-to-face π stacking with one of the ring benzo groups.

The X-ray structure of the di-Boc protected intermediate **1** was also obtained and shows the presence of two independent molecules in the unit cell (Supporting Information, Figure S5). Both molecules correspond to the connectivity predicted from the physical measurements and, not unexpectedly, show that the macrocyclic ring conformation in each structure differs considerably from that found for protonated $\mathbf{L}^1$, with the three tertiary nitrogen donors orientated exo to the cavity in each case.

In addition, an X-ray structure analysis was undertaken using poor quality red crystals of $\mathbf{L}^2 \cdot 2HNO_3$ (Supporting Information, Figure S6). The resulting determination was not of high quality but was adequate to confirm the expected atom connectivity and show that this compound also crystallizes in two crystallographically independent forms, each with similar configurations, in an antiparallel arrangement. Evidence for intermolecular π-π stacking between adjacent structures via their benzo-aza groups is present.

Dye-Attached Macrocycle $\mathbf{L}^2$ − Solution and Solid State Studies. A number of chromoionophoric systems based on metal-ion induced charge-transfer phenomena have now been reported, including systems employing macrocyclic rings as the metal-binding site.[14] We now report a further study of this type employing the azo-macrocyclic derivative $\mathbf{L}^2$. It is noted that the dye-attached system $\mathbf{L}^2$ has a similar macrocyclic metal coordination domain to that in $\mathbf{L}^1$, and hence parallel metal binding behavior is expected for both these ligands. The UV−vis spectrum of $\mathbf{L}^2$ in acetonitrile is characterized by an intense band (ε = 23000 M^{-1} cm^{-1}) centered at 495 nm, giving rise to a red solution. The interaction of this ligand with Co(II), Ni(II), Cu(II), Zn(II), Cd(II), Hg(II), Pb(II), and Ag(I) was investigated by monitoring changes in the UV−vis spectra of $\mathbf{L}^2$ in aceto-

(13) (a) Adam, K. R.; Lindoy, L. F.; Lip, H. C.; Rea, J. H.; Skelton, B. W.; White, A. H. *J. Chem. Soc., Dalton Trans.* **1981**, 74. (b) Price, J. R.; Fainerman-Melnikova, M.; Fenton, R. R.; Gloe, K.; Lindoy, L. F.; Rambusch, T.; Skelton, W.; Turner, P.; White, A. H.; Wichmann, K. *Dalton Trans.* **2004**, 3715. (c) Gasperov, V.; Galbraith, S. G.; Lindoy, L. F.; Rumbel, B. R.; Skelton, B. W.; Tasker, P. A.; White, A. H. *Dalton Trans.* **2005**, 139.

(14) (a) Misumi, S.; Kaneda, T. *J. Inclusion Phenom. Mol. Recognit. Chem.* **1989**, *7*, 83. (b) Löhr, H.-G.; Vögtle, G. *Acc. Chem. Res.* **1985**, *18*, 65. (c) Izatt, R. M.; Pawlak, K.; Bradshaw, J. S. *Chem. Rev.* **1991**, *91*, 1721. (d) Badaoui, F. Z.; Bourson, J. *Anal. Chim. Acta* **1995**, *302*, 341. (e) Kim, J. S.; Shon, O. J.; Lee, J. K.; Lee, S. H.; Kim, J. Y.; Park, K.-M.; Lee, S. S. *J. Org. Chem.* **2002**, *67*, 1372. (f) Descalzo, A. B.; Martínez-Máñez, R.; Radeglia, R.; Rurack, K.; Soto, J. *J. Am. Chem. Soc.* **2003**, *125*, 3418. (g) Boiocchi, M.; Fabbrizzi, L.; Licchelli, M.; Sacchi, D.; Vázquez, M.; Zampa, C. *Chem. Commun.* **2003**, 1812. (h) Wager-Wysiecka, E.; Luboch, E.; Kowalczyk, M.; Biernat, J. F. *Tetrahedron* **2003**, *59*, 4415. (i) Lee, S. J.; Jung, J. H.; Seo, J.; Yoon, I.; Park, K.-M.; Lindoy, L. F.; Lee, S. S. *Org. Lett.* **2006**, *8*, 1641. (j) Lee, H. G.; Lee, J.-E.; Choi, K. S. *Inorg. Chem. Commun.* **2006**, *9*, 582.

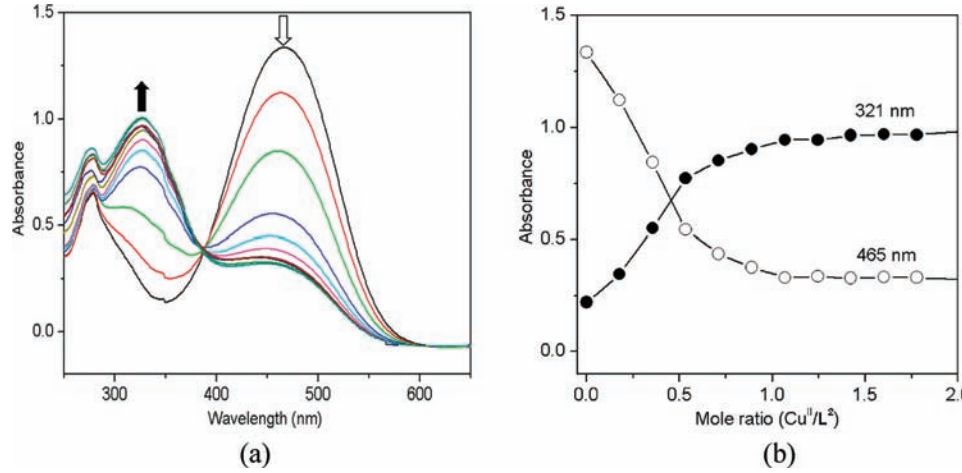

Figure 5. UV−vis titrations of $\mathbf{L}^2$ (5.0×10^{-5} M) with Cu(II) nitrate (0−2.5 equiv) in DMSO: (a) spectral changes and (b) titration curves.

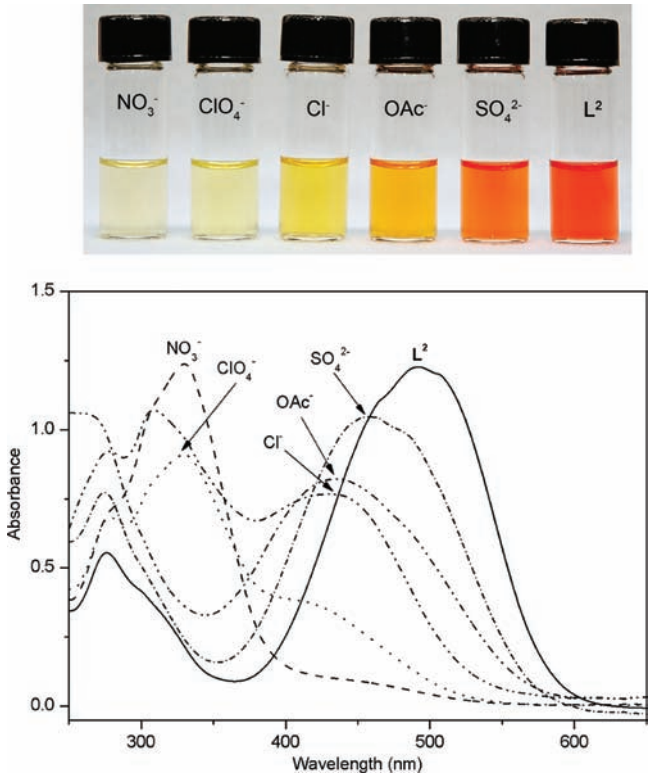

Figure 6. Changes in the UV−vis spectrum of $\mathbf{L}^2$ on addition of the Cu(II) salts in acetonitrile (ligand concentration, 5.0×10^{-5} M; added metal ion, 3.0 equiv).

Table 3. Selected Bond Lengths (Å), Bond Angles (deg), and Torsion Angles (deg) for **6**

Cu1−N1	2.007(5)	Cu1−N2	2.081(5)
Cu1−N3	2.007(5)	Cu1−O7	1.972(4)
N1−Cu1−N2	86.4(2)	N3−Cu1−N2	86.3(2)
N3−Cu1−N1	150.1(2)	O7−Cu1−N1	96.11(19)
O7−Cu1−N2	177.3(2)	O7−Cu1−N3	92.0(2)
N1−C9−C10-N2	51.9(7)	N2−C11−C12−N3	53.5(7)

nitrile on addition of each of these ions as their metal nitrate salts. The spectrophotometric changes are shown in Figure 4; in each case there is a hypochromic shift[14] in the absorption maxima (λ_{max}) upon metal complexation and a concurrent reduction in molar absorptivity; the largest λ_{max} shift (to 321 nm; $\Delta\lambda_{max} = 174$ nm) is induced by Cu(II) resulting in a solution color change from red to pale-yellow.

Table 4. Selected Bond Lengths (Å), Bond Angles (deg), and Torsion Angles (deg) for **7**

Cu1−N1	2.031(5)	Cu1−N3	2.027(5)
Cu1−O9	1.921(4)	Cu1−O9A	1.918(4)
N3−Cu1−N1	94.5(2)	O9−Cu1−N1	95.56(19)
O9[a]−Cu1−N1	173.03(19)	O9−Cu1−N3	169.41(19)
O9[a]−Cu1−N3	92.2(2)	N1−C9−C10−N2	−57.0(7)
N2−C11−C12−N3	−53.5(9)		

[a] Symmetry operation: $-x + 1, -y + 2, -z$.

In an attempt to probe the origins of the above observed spectrophotometric changes, the solution behavior of selected complexes of $\mathbf{L}^2$ was investigated in further detail. In particular, spectrophotometric titration of $\mathbf{L}^2$ with Cu(II) nitrate (Figure 5a) was carried out in DMSO; in this case the ligand absorption at 465 nm gradually decreased while the complex absorption centered at 321 nm increased giving rise to a corresponding isosbestic point at 390 nm. According to the titration curves in Figure 5b, both for the ligand (465 nm) and complex (321 nm) absorptions, the spectral features are consistent with a 1:1 binding ratio between Cu(II) and ligand. The Job plots for $\mathbf{L}^2$ complexation with Cu(II) and Ni(II) also indicated 1:1 stoichiometries (Supporting Information, Figure S7).

While investigating the metal-ion complexation and metal-induced color changes for $\mathbf{L}^2$ discussed above, a spectral dependence on the anion employed was observed in individual cases. To probe this effect further, changes in the UV−vis spectra of $\mathbf{L}^2$ were recorded on the addition of Cu(II) as its chloride, nitrate, perchlorate, acetate, and sulfate salts. In each case a blue shift (and corresponding color change) was observed (Figure 6). These anion-induced shifts to lower wavelength fall in the order NO_3^-, ClO_4^- > Cl^-, OAc^- > SO_4^{2-}. While it is noted that this order shows correlation with the Hofmeister series of relative anion lipophilicities,[15] it is difficult to offer a convincing rationale for such a trend in the absence of detailed information concerning the respective solution structures involved. For example, the above sequence does not follow the expected relative binding strengths of these anions for Cu(II); thus the relatively weak coordinating ClO_4^- has a larger effect than the more strongly

(15) (a) Hofmeister, F. *Arch. Exp. Pathol. Pharmakol.* **1887**, *24*, 247. (b) Morf, W. E.; Simon, W. *Helv. Chim. Acta* **1986**, *68*, 1120.

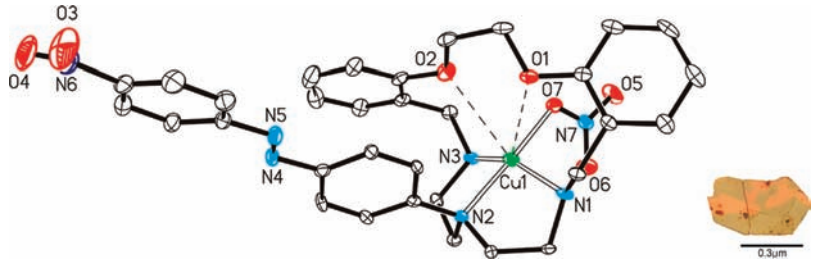

Figure 7. Endo-coordinated structure of **6**, $[Cu(\mathbf{L}^2)NO_3]NO_3 \cdot CH_2Cl_2$ (pale-yellow crystals). Hydrogen atoms, non-coordinating anions and solvents are omitted.

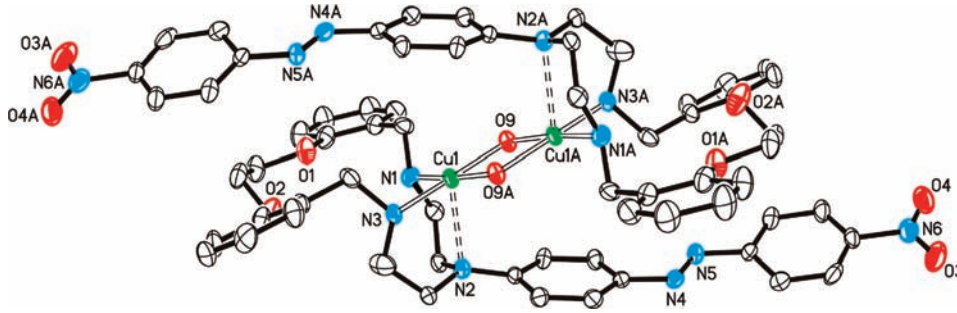

Figure 8. Exo-coordinated dimeric structure of **7**, $[\{Cu(\mathbf{L}^2)\}_2(\mu\text{-}OH)_2](ClO_4)_2 \cdot 2CH_2Cl_2 \cdot 2H_2O$ (dark-red crystals). Hydrogen atoms, non-coordinating anions, and solvents are omitted.

binding Cl^- anion. Clearly, the situation appears more complicated than simply reflecting anion coordination to the Cu(II) center. Nevertheless, a related anion influence has been noted previously for a *N*-chromogenic calix[4]azacrown system.[14e]

X-ray structures of the Cu(II) nitrate (**6**) and Cu(II) perchlorate (**7**) complexes of $\mathbf{L}^2$ have been obtained. In the case of complex **6**, the X-ray analysis confirmed a 1:1 species of type $[Cu(\mathbf{L}^2)NO_3]NO_3 \cdot CH_2Cl_2$ (Figure 7 and Table 3) in which the Cu(II) ion has a pseudo six-coordinate environment, with the copper being bound to the three nitrogen donors of $\mathbf{L}^2$ and an oxygen from a bound monodentate nitrato ligand; two ether oxygens from the macrocyclic ligand also interact weakly with the copper: Cu1−O1 3.048, Cu1−O2 2.912 Å. The second nitrate anion is not coordinated (Cu1···O10 4.333 Å, not shown). The presence of the Cu1−N2 bond [2.081(5) Å] involving the tertiary nitrogen with attached azo-substituent is undoubtedly important in inducing the observed color change from red in the free ligand to pale-yellow for the present complex; in this category of chromoionophore, it is the net electronic charge transfer from the donor group (tertiary nitrogen) to the acceptor group (the benzo-aza chromophore) that will influence the color of the chromophore.[14]

Next, the reaction of $\mathbf{L}^2$ with Cu(II) perchlorate yielded dark-red crystals of **7** whose X-ray analysis confirmed a dimeric structure of type $[\{Cu(\mathbf{L}^2)\}_2(\mu\text{-}OH)_2](ClO_4)_2 \cdot 2CH_2Cl_2 \cdot 2H_2O$ (Figure 8 and Table 4). Since there is an imposed inversion at the center of the two copper atoms, the asymmetric unit contains one molecule of $\mathbf{L}^2$, one copper atom, one hydroxide ion, and one perchlorate ion (not shown).[16] The structure contains a rhomboidal Cu-$(OH)_2$-Cu core connecting two bound macrocycles. Each Cu(II) is five-coordinate being bound to three exo-oriented secondary amine nitrogens from one macrocyclic ring and the two bridging OH^- groups; both macrocyclic rings adopt a bent configuration. As found for the Cu(II) complexes of other related O_2N_3-donor macrocycles of the present type, the macrocyclic oxygen donors of each macrocycle in the dimeric arrangement do not coordinate.[13a,c,17] The tertiary (anilino) amine N2 occupies an axial position with respect to the square-plane to yield an overall distorted square-pyramidal coordination geometry. It is noteworthy that the Cu1−N2, (2.519(5) Å) bond distance in **7** is much longer than occurs for the corresponding bond in **6** [Cu1−N2, 2.081(5) Å]. This weaker coordination in the fifth (axial) position [Cu1−N2, 2.519(5)] in the latter case can in part be rationalized in terms of the dominance of the strongly bound rhomboidal Cu-$(OH)_2$-Cu core on copper complexation resulting in weaker Cu1−N2 bond formation. In parallel with this, only a very minor color change of the solid state complex is observed relative to that of the uncomplexed ligand. These results demonstrate how variation of the macrocyclic ring coordination mode, which corresponds to endo coordination in **6** but exo in **7**, markedly influences the strength of binding of the tertiary nitrogen containing the pendent azo function and which, in turn, is reflected by the respective colors of the individual complexes. Thus clearly the above results demonstrate that the color of the pendent phenylaza chromophore is markedly dependent on the strength of metal binding of the attached nitrogen donor. Nevertheless, it is important to note that the similarity of the solution spectra of the nitrate and perchlorate species (Figure 6) relative to the different colors of the solid state complexes strongly suggests, at least in the case of the perchlorate species, that the solid state and solution structures are different under the conditions employed, perhaps reflecting the relatively

(16) Kuzelka, J.; Mukhopadhyay, S.; Springler, B.; Lippard, S. J. *Inorg. Chem.* **2004**, *43*, 1751.

(17) Baldwin, D. S.; Duckworth, P. A.; Leong, A. J.; Lindoy, L. F.; McPartlin, M.; Tasker, P. A. *J. Chem. Soc., Dalton Trans.* **1993**, 1013.

stronger affinity of nitrate over perchlorate for the copper(II) center, especially with respect to the solid state.

Conclusion

In this report, the complexation of Cu(II) with selected N_3O_2-donor macrocyclic rings has been explored. One such system, $\mathbf{L^2}$, incorporating a pendant benzo-diazonium center has been demonstrated to undergo metal-dependent hypochromic shifts in its electronic spectrum, with strongly bound copper inducing the largest shift. X-ray studies have assisted in defining the structure−function relationship underlying the observed color change of red to yellow in this case. In seven-metal competitive transport experiments across bulk chloroform membranes, $\mathbf{L}^1$ and $\mathbf{L}^3$ were demonstrated to yield sole selectivity for Cu(II) over the remaining six transition and post transition metal ions present in the aqueous phase. When compared on an "available macrocyclic cavity" basis, the linking of macrocyclic rings resulted in decreased metal ion extraction efficiency relative to related single-ring ligand systems.

Acknowledgment. S.S.L. thanks the financial support from the Korea Research Foundation (2007-314-C00157). L.F.L. thanks the Australian Research Council for support.

Supporting Information Available: X-ray crystallographic files in CIF format and NMR and mass data. This material is available free of charge via the Internet at http://pubs.acs.org.

IC801265Y